THE SPECTRAL ENERGY DISTRIBUTION OF STARS ON THE BROADBAND PHOTOMETRY

N. Z. Ismailov [a*], ***A. F. Kholtygin*** [d**], ***I. I. Romanyuk*** [b], ***M. A. Pogodin*** [c]

[a] *Shamakhy Astrophysical Observatory named after N.Tusi, Azerbaijan National Academy of Sciences, Shamakhy region, Azerbaijan*

[b] *Special Astrophysical Observatory of the Russian Academy of Sciences, Nizhny Arkhyz, Karachay-Cherkess Republic, Russia, 369167*

[c] *Main Astronomical Observatory of the Russian Academy of Sciences in Pulkovo, Pulkovskoe shosse 65, 196140, St. Petersburg, Russia*

[d] *Saint Petersburg State University, Faculty of Mathematics and Mechanics, Department of Astronomy, Saint Petersburg, Russia*

The method used in this work for carrying out the spectral energy distribution of stars from the data of broadband photometric values in the spectral range of 0.36-100 μm is described.For this, we used the results of multicolor photometric observations in the UBVRIJHK system, as well as data from the WISE and IRAS catalogs. Data from different catalogs are transformed into fluxes in the CGS system of units. In an accessible form for the catalogs under consideration, the values of the photometric zero point fluxes are given. This technique was applied for testing standard stars, as well as for stars that have a gas or gas-dust disks: the Herbig Ae/Be stars, Be, α Lyr type, as well as for a pair of stars from the Orion Nebula Ori OB1. It is shown that stars from the Ori1 complex HD 33917 and HD 36629 have significant excesses of radiation in the far-IR range. It is assumed that such an excess of radiation perhaps is formed in the dusty of the remnant circumstellar discs.

Keywords: Optical and IR photometry–stellar energy distribution–circumstellar disks–IR excess of radiation.

* E-mail: ismailovnshao@gmail.com
** E-mail: afkholtygin@gmail.com

1. INTRODUCTION

The spectral energy distribution (SED) of stars is one of the most important characteristics of their radiation. Determination of the main physical parameters of stellar atmospheres, such as temperatures, gravitational acceleration, agents that absorb radiation or excess radiation in the continuous spectrum, chemical composition, is carried out by using the energy distribution. The anomalous distribution of energy in certain parts of the star's spectrum can be revealed by comparing it with the models of photospheres built for normal stars. This makes it possible to establish the physical phenomena due to which such anomalies are occurred.

Infrared (IR) radiation is a very important part of the radiation spectrum of stars. Infrared studies allow viewing the contents and structure of the Galaxy, the structure of star-forming regions and the circumstellar environment. It is relatively free of interstellar extinction, which makes it difficult to measure at shorter wavelengths. Since the nature of the brightest sources in the sky varies with the wavelength of infrared radiation, and most of them are variable objects, for complete information it is necessary to study the radiation of objects at a long wavelength.

It is known that, for example, stars with a circumstellar gas and dust disk have significant infrared (IR) radiation in the near and far IR spectral regions. Such examples are T Tauri and Ae/Be Herbig type stars, Be stars, Vega stars, etc. [1, 2]. The nature of the emission of the circumstellar disk in the IR part of the spectrum can provide comprehensive information about the physics and structure of the circumstellar disks in these objects. This makes it possible to estimate their physical parameters and study the stages of planet formation in circumstellar disks at different stages of stellar evolution.

In this paper, we describe a technique for plotting the SED curves of different stars based on the data of broadband photometric observations.

2. APPLIED PROCEDURE

One of the methods for plotting the SED curves in a wide spectral range is based on the use of observational data of multicolor photometry. In this work, we will describe in detail the method for plotting the SED curves of stars based on the data of the international broadband UBVRIJHKLM photometry. In addition, data from the Wide-field Infrared Survey Explorer (WISE) [3], Infrared Astronomical Satellite (IRAS) [4] catalogs, and Diffuse Infrared Background Experiment (DIRBE / COBE) [5] about which we will write below. In conclusion, we give examples of the constructed SED curves for different test stars.

2.1. Multi-color photometric system

The multicolor photometric system UBVRIJHKLM was formed on the basis of the classic UBV Johnson system [6], and then, with the development of technology for the production of light detectors in the IR part of the spectrum, it was supplemented with different filters that allow covering the wavelength range $\lambda \sim 0.36 - 34\mu m$ [7]. We will not describe in detail on this characteristics of this photometric system and will only present the methodology by which we plotted the SED curves. Table 1 shows the effective wavelengths of different bands in microns and the adapted absolute radiation fluxes of a zero-magnitude star of spectral type A0V, given in [7]. As you can see, with the use of these bands it is possible to cover the spectral range of 0.36 - 34 μm. In addition, depending on the task of the study, with the involvement of archival observational data from different space missions, this range can be significantly expanded.

The principle of plotting the SED curves for different objects based on the magnitudes obtained in different bands of broadband photometry consists in converting the magnitudes of m_λ into absolute fluxes F_λ according to the well-known expression

$$F_\lambda = F_0 \cdot 10^{-0.4(m_\lambda - m_0)} \quad (1)$$

Here F_0 is the adapted radiation flux for the zero-point of the system, when m_0 is taken equal to zero. The referencing is usually performed to the adapted absolute flux radiation of a standard zero-magnitude star A0V in all emission bands [7]. The star Vega can be such a standard with a certain approximation. Table 1. Radiation fluxes from the star A0V of zero magnitude in different bands in the extended Johnson system. Below is presented the transformational characteristics of WISE systems.

Table 1: Radiation fluxes from the star A0V of zero magnitude in different bands in the extended Johnson system. Below is presented the transformational characteristics of WISE systems.

	$\lambda_0(\mu m)$	F_λ $(ergs^{-1}sm^{-2}$ Å$^{-1})$		$\lambda_0(\mu m)$	F_λ $(ergs^{-1}sm^{-2}$ Å$^{-1})$
U	0.36	$4.22 \cdot 10^{-9}$	L	3.5	$7.1{\cdot}10^{-12}$
B	0.44	$6.40{\cdot}10^{-9}$	M	5.0	$.0 \cdot 10^{-12}$
V	0.55	$3.75 \cdot 10^{-9}$	N'	8.4	$2.4 \cdot 10^{-13}$
R	0.71	$1.75 \cdot 10^{-9}$	N	10.4	$1.1 \cdot 10^{-}13$
I	0.97	$8.4 \cdot 10^{-10}$	N"	10.7	$9.8 \cdot 10^{-14}$
J	1.25	$3.1 \cdot 10^{-10}$	O	11.0	$8.5 \cdot 10^{-14}$
H	1.62	$1.2 \cdot 10^{-10}$	P	12.2	$6.6 \cdot 10^{-14}$
K	2.2	$3.3 \cdot 10^{-11}$	Z	34.0	$8.8 \cdot 10^{-16}$
W1	3.4	$8.178 \cdot 10^{-12}$	W3	11.6	$6.515 \cdot 10^{-14}$
W2	4.6	$2.415 \cdot 10^{-12}$	W4	22.1	$5.09{\cdot}10^{-15}$

Before converting stellar magnitudes into fluxes, it is necessary to know the interstellar reddening coefficient for each star and the available stellar magnitudes for each photometric bands must be cleared of interstellar reddening. In catalogs, you can often find the reddening factor in the V-band Av, or the so-called color excess index E (B-V). Color excess E (B-V) is determined by the ratio

$$E(B-V) = B - V(B-V)_0 \tag{2}$$

Here B-V is the observed color index of the star, and $(B-V)_0$ is the color index of a standard star free from interstellar reddening with the same spectral and luminosity classes. There are special tables compiled from numerous empirical data and consistent with theories of stellar atmospheres, which give normal color indexes for different spectral classes of stars (see, for example, [7, 8]). The interstellar extinction Av is determined by the expression.

$$A\nu = R \cdot E(B-V) \tag{3}$$

For the normal interstellar reddening law, the coefficient is R $\sim$ 3.1. Within the wavelength range less than 3.5 mm, the interstellar reddening law is basically the same [9]. To determine the value of interstellar absorption for any other wavelength A_λ, one can apply the formula

$$A_\lambda / E(B-V) = E(\lambda - V)/E(B-V) + R \tag{4}$$

In the regions of about 3.5 mm and at long wavelengths, silicate absorption increases, and the character of the interstellar reddening distribution law becomes more complicated. Table 2 shows the value of interstellar extinction for different wavelengths in a multicolor system for the interval 0.36–13 μm [10]. Knowing the value of Av, we can determine A for any other wavelength, with respect to the ratio A_λ/Av from Table 2. The table was compiled according to the review data of the authors [11–13].As can be seen from Table2, already at $\lambda \leq 1\mu m$, the value of A_λ becomes much less.

2.2. WISE catalogue data

Table 1. shows the effective wavelengths of the photometric bands of the WISE catalog system (NASA). The effective wavelengths of the filters are 3.4, 4.6, 12 and 22 μm (W1, W2, W3, W4). For point sources in undistorted sky regions of galactic dust, the sensitivity of individual bands at the 5 level is 0.08, 0.11, 1, and 6 mJy, respectively. In the WISE catalog, data are given in magnitudes, so we need to transform these magnitudes into to fluxes.

To calibrate the zero point of this system to absolute flux, the mission website (https://wise2.ipac.caltech.edu/docs/release/allsky/e.psup/sec4_4h.htmlWISEZMA)

Table 2: Interstellar reddening law

λ	E(λ-V)/E(B-V)	$A_\lambda/A\nu$	Van de Hulst No15
	1.64	1.531	1.555
	1.00	1.324	1.329
	0.0	1.000	1.000
	-0.78	0.748	0.738
	-1.6	0.482	0.469
	-2.22±0.02	0.282	0.246
	-2.55±0.03	0.175	0.155
	-2.744±0.024	0.112	0.0885
	-2.91±0.03	0.058	0.045
	-3.02±0.03	0.023	0.033
	-2.93	0.052	0.013
8	-3.03	0.020±0.003	
8.5	-2.96	0.043±0.006	
9.0	-2.87	0.074±0.011	
9.5	-2.83	0.087±0.013	
10.0	-2.86	0.083±0.012	
10.5	-2.87	0.074±0.011	
11	-2.91	0.060±0.009	
11.5	-2.95	0.047±0.007	
12	-2.98	0.037±0.006	
12.5	-3.00	0.030±0.004	
13	-3.01	0.027±0.004	

provides the following coefficients for bands 3.4, 4.6, 12 and 22 μm: $8.178{\cdot}10^{-15}Wsm^{-2}\mu m^{-1}, 2.4\,15{\cdot}10^{-15}Wsm^{-2}\mu m^{-1}, 6.515{\cdot}10^{-17}Wsm^{-2}\mu m^{-1} and$ $5.09 \cdot 10^{-18}Wsm^{-2}\mu m^{-1}$, respectively. It is easy to express these flows in angstroms, and then we get the necessary zero-point coefficients for the transition to absolute fluxes:

$$\begin{aligned}
(\mathrm{FW_W})_0 &= 8.178 \cdot 10^{-12}\ \mathrm{erg\ s^{-1}\ sm^{-2}\ A^{-1}} \\
(\mathrm{FW2})_0 &= 2.415 \cdot 10^{-12}\ \mathrm{erg\ s^{-1}\ sm^{-2}} A^{-1} \\
(\mathrm{FW3})_0 &= 6.515 \cdot 10^{-14}\ \mathrm{erg\ s^{-1}\ sm^{-2}\ A^{-1}} \\
(\mathrm{FW})_0 &= 5.09 \cdot 10^{-15}\ \mathrm{erg\ s^{-1}\ sm^{-2}\ A^{-1}}
\end{aligned} \tag{5}$$

These values are also shown in Table 1. Thus, knowing the transformation ratios (4), one can easily transform the stellar magnitudes listed in the WISE catalog into absolute fluxes.

2.3. Data's of catalogs IRAS and DIRBE

To supplement the SED curves of program stars in the far IR range of the spectrum, we used the photometric data from the IRAS mission catalogue (USA, England, and the Netherlands) (https://irsa.ipac.caltech.edu/IRASdocs/iras.html) given in the following effective lengths waves: 12, 25, 60 and 100 microns, respectively. The flux densities radiation in these bands are given in the off-system unit Jansky (Jy), so we have to translate them into the more popular and familiar flux unit in the CGS system in erg $s^{-1}sm^{-2}$ Å^{-1}.
To carry out such a transfer, we need to calculate the transformation ratios for each of the four bands. Since the unit Jy in the CGS system is expressed in frequency by the following ratio, $1Jy = 10 - 23\, ergs^{-1}sm^{-2}Hz^{-1}$, to convert to wavelengths in Å, we must to calculate the flux corresponding to the per unit of frequency. From the known relation for the elementary range of wavelengths $\delta\lambda$ and frequency $\delta\nu$, one can write

$$v = \frac{\mathrm{c}}{\lambda}, \quad \partial v = -\frac{\mathrm{c}}{\lambda^2}\partial\lambda \Rightarrow \frac{\delta\lambda}{\delta v} = -\frac{\lambda^2}{c} \tag{6}$$

After calculating the value $\frac{2}{c}$ from expression (5), the reduced flux density in Jy must be divided by this value.The minus sign means that as the wavelength increases, the frequency decreases. For example, for the band $\lambda = 120,000$ Å$= 2\,\mu m$ we can get Then for this band we can get relation.

$$\left|\frac{\delta\lambda}{\delta v}\right| = \frac{(1.2\cdot 10^5)^2}{3\cdot 10^{18}\text{Å}s^{-1}} = \frac{1.44\cdot 10^{10}\text{Å}^2}{3\cdot 10^{18}\text{Å}\cdot Hz} = 0.48\cdot 10^{18}\text{Å}\cdot \text{Hz}^{-1}$$

$$1\text{Jy} = 10^{-23}\ \text{erg s}^{-1}\text{sm}^{-2}\ \text{Hz}^{-1}/0.48{\cdot}10^{18}\ \text{A}{\cdot}\text{Hz}^{-1} = 2.08{\cdot}10^{-15}\ \text{erg s}^{-1}\ \text{sm}^{-2}\ \text{A}^{-1} \tag{7}$$

Similarly, we can calculate coefficient for the transformation 1 Jy for the rest of the bands. Table 3 gives this value for magnitudes given in different bands.
As is known, the near-IR survey was first carried out in the Two Micron Sky Survey (TMSS [14]), and later, by the Two Micron All Sky Survey (2MASS [15]) and DENIS [16] missions. The IRAS survey covered the 12-100 μm interval [17]. The intermediate spectral interval was covered by the Midcourse Space Experiment (MSX) [18] and Air Force Geophysical Laboratory (AFGL) Infrared Sky Survey [19] missions. Observations of these missions differ in sensitivity and scale of sky

coverage.

There is another unused infrared database suitable for cataloging point sources of infrared radiation: archived data from the Diffuse Infrared Background Experiment (DIRBE [20]) on the Space Background Explorer (COBE [21]). DIRBE operated at cryogenic temperatures for 10 months in 1989-1990, providing full sky coverage at 10 infrared wavelengths (1.25, 2.2, 3.5, 4.9, 12, 25, 60, 100, 140 and 240μm).

Although DIRBE was developed to search for cosmic infrared background, the data is also used to study point sources (see, for example, [22]), despite the fact that it has a relatively low spatial resolution (0.7°). Since the data of the DIRBE catalog are given in units of Jy, similarly to the transformation of the IRAS data, these data must be converted to erg $s^{-1}sm^{-2}$ Å^{-1}. We carried out such a translation for all DIRBE bands; the results are also shown in Table 2. Since the DIRBE catalog does not contain data on the bands of 140 and 240 μm (which would be very useful for our work) for our program stars, we did not use these data in our diagrams. The description here of this catalogues is purely methodical.

Table 3: Coefficients of transformation of the off-system flux radiation unit of Jansky into the CGS system for IRAS and DIRBE / COBE data.

IRAS and DIRBE/COBE (transformation coefficients from Jy to erg $s^{-1}sm^{-2}$Å^{-1})					
	$\lambda_0(mkm)$	$F_\lambda(erg\,s^{-1}sm^{-2}$ Å$^{-1})$		λ_0 (mkm)	F_λ $(ergs^{-1}sm^{-2}$ Å$^{-1})$
[1.25]	1.25	$1.92 \cdot 10^{-13}$	[25]	25	$4.81 \cdot 10^{-16}$
[2.2]	2.2	$1.20 \cdot 10^{-14}$	[60]	60	$8,33 \cdot 10^{-17}$
[3.5]	3.5	$2.44 \cdot 10^{-14}$	[100]	100	$3.00 \cdot 10^{-17}$
[4.9]	4.9	$1.25 \cdot 10^{-14}$	[140]	140	$1.53 \cdot 10^{-17}$
[12]	12	$2.08 \cdot 10^{-15}$	[240]	240	$5.21 \cdot 10^{-18}$

Since many bands of the part of the Johnson system modified for the IR [6] also cover the intermediate range of the IR region, for homogeneity in what follows we will use only the data of the UBVRIJHK [3], WISE [29] and IRAS [28] systems, which allow us to cover the spectral range from 0.36 μm to 100 μm.

Note that there are sites that online can convert flaxes into the desired unit form (see, for example, https://www.gemini.edu/sciops / instruments / midir-resources / imaging-calibrations / flu.-conversion-tool, and also https://www.nebulousresearch.org/codes/flu.units). In the latter site, you can check your calculations to make sure that the units are converted correctly.

It should be noted that the IRAS catalogue data are distorted by certain factors that significantly affect the results of observations (https://irsa.ipac.caltech.edu/applications/DUST/).The data on the inter-

stellar dust of the galaxy are especially strongly distorted, due to which the measurement errors in different coordinates can exceed by 100% the value itself. For example, for one of our stars, HD 33917, using a special IRAS server, we determined that the distortions in 1998 in individual bands reached from 0.0877 to 0.0935 Jy (see also [23]), and in 2011 from 0.27 to 0.32 Jy (see also [24]), which are practically equal to the measured value itself.

3. PLOTTED EXAMPLES OF SED CURVES

To check the correctness of the applied method and the performed calculations, we plotted the SED curves of standard stars for test and for stars with different circumstellar characteristics. In [25], it is shown that the star Vega has a faint envelope, or a dust ring, which is revealed only at 60–100 μm. The authors attributed this radiation to dust particles over a millimeter in size and a temperature of about 85 K.

In [26], a list of stars that are located at a distance of 25 pc from the Sun is given. Among them, the authors found 12 Vega-like stars out of 36, and all 12 stars have excess radiation in the bands of 60 and 100 μm, which, like Vega, is explained by the presence of a dust envelope.

As test stars, we used standard stars, which are given in [25, 26]. Figure 1 shows examples of the SED curves for standard stars α Car and α Leo. Here, and in the following figures, the dotted line shows the black body (BB) radiation curve corresponding to the effective temperature of the star, determined from the spectral type. The solid curve shows the approximation in the wavelength range of 0.36-20 μm according to the Kurucz models [27]. For the values of the flux densities, both in the Kurucz model and in the blackbody radiation, only those flux values were used that were corresponding to the wavelengths of the used photometric bands. The lower panels in Fig.1. is shown the dependence of log F^*/F_0 on the wavelength, where F^* is the observed radiation flux from the star, F_0 is the radiation flux according to the Kurucz model at the same wavelength. Since we could apply the model only up to a wavelength of 20 μm [27], the BB radiation curve with the corresponding temperature was used for approximation the rest of the spectrum to 100 μm. As can be seen from the lower panels in Fig. 1, no excess emission is observed in the tested standard stars, and therefore the value of log F^*/F_0 with a certain scatter $\pm\sigma$ is close to zero. In the lower parts of each panel, dashed lines show the approximation error of $\pm 3\sigma$ for each distribution at $\sigma = \pm 0.07$.

Fig. 2 shows the SED curves of the Herbig Ae/Be star HD 179218 (upper right panel) and typical star Be γ Cas (upper left panel). As is known, Be stars have gaseous disks, which give excess radiation in the IR range. In Ae/Be Herbig stars, the excess radiation can be explained by the gas and dust disk radiation. It can be seen that the far IR excesses in Ae/Be H stars can be approximated by the emission of matter with temperatures from 50K to 1000K (lower panels in Fig. 2).

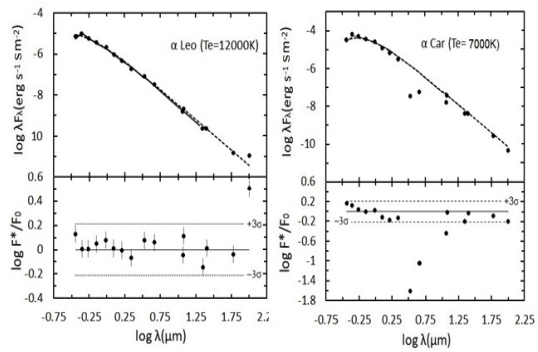

Fig. 1: Examples of SED curves for test stars α Car (top left) and α Leo (top right). Solid curves - Kurucz model, dashed lines - blackbody radiation. In the lower parts of each panel, dashed lines show the mean approximation error of $\pm 3\sigma$ for each distribution at $\sigma = \pm 0.07$.

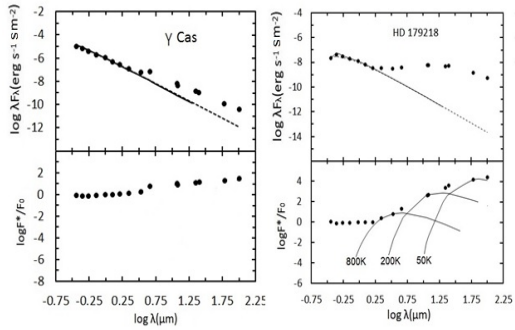

Fig. 2: Examples of SED curves for the Be star γ Cas (top left) and the Herbig AeBe star HD179218 (top right). The solid line indicates the approximation according to the Kurucz model, the dotted line indicates the BB radiation. In the lower panels of figure, the area of excess radiation is showed, which in case HD 179218 was approximated by the blackbody radiation of different temperatures indicated in the figure.

In the Figure 3. is shown the SED curve for the stars α Lyr and AB Aur. The obtained SED curve for α Lyr confirms the result of the authors of [25], who found an insignificant excess in the far IR range. The young star Ae Herbig AB Aur has an extensive disk of gas and dust, which is in good agreement with the literature data (see, for example, [30]).

On the Figure 4. is demonstrated the SED curves for two stars HD 33917 (sp A0V) and HD36629 (sp B2V) from the list given in [31]. The stars are pleased in the young

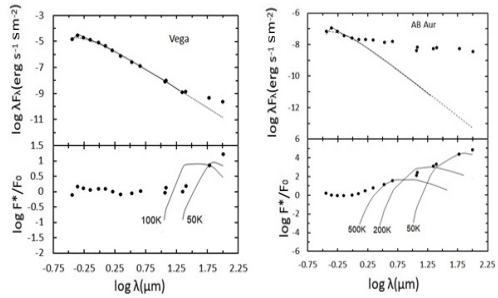

Fig. 3: Examples of SED curves for test stars α Lyr (top left) and AB Aur (top right). Solid curves - Kurucz model, dashed lines - blackbody radiation. The lower parts of each panel show the dependence of log F^*/F_0 on the wavelength. The curves show the approximation corresponding to the blackbody radiation at different temperatures.

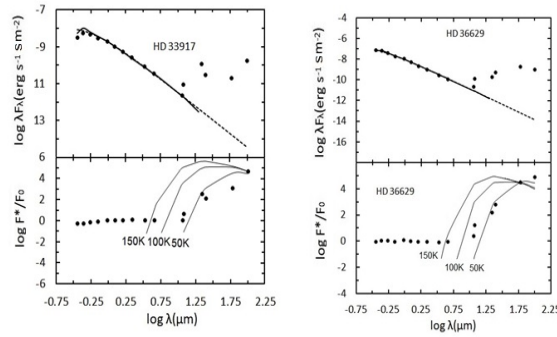

Fig. 4: Examples of SED curves of stars from Orion starformation region. The designations are the same as in Figures 2-4.

star-forming complex Ori OB1 in the Orion Nebula. As can be seen, these stars showed a significant deviation from the model distribution, mainly in the region of 60-100 microns. The maximum IR radiation is achieved in the 100 μm band. It can be seen in the lower panels in Fig 3. that the observed IR excesses can be approximated with the emissions from the blackbody with a temperature of about 50K-80K.

4. CONCLUSIONS

Thus, in this work, we described in detail the method for plotting the SED curves of stars in the spectral range from 0.36 to 100 μm from the data of observations of broad-

band photometry. The technique also allows us to study the distribution of the radiation flux of various space objects, stars, galaxies, etc. The plotted SED curves for a group of test stars showed consistent results with those obtained earlier for these stars.

For two BA stars from the Orion Nebula Ori OB1 star formation complex, it was shown that these stars exhibit excess of IR radiation in the 25-100 μm region, which indicates the existence of dust around these stars with a temperature of about 80-100K. The belonging of these two stars to the Orion complex Ori OB1 is beyond doubt. This means that these stars from the Ori OB1 complex have passed a significant evolutionary path and are at the final stage of dissipation of the circumstellar disks. It is known that the ages of the stellar population of the Ori OB1 complex should be in the order of $10^5 - 10^6$ years. The detection of cold circumstellar dust in BA stars is also one of the main common features of Ae/Be Herbig stars. Therefore, it can be assumed that the stars from the Ori OB1 complex HD 33917 and HD36629 are at an older stage of evolution than the Herbig Ae/Be stars. At the same time, it can be assumed that young stars of intermediate mass at a certain stage of evolution can be turn into α Lyr type stars. To clarify the validity of this hypothesis, additional studies of the characteristics of individual BA stars located in young star-forming complexes are required.

ACKNOWLEDGEMENTS

This work was supported by the Science Development Foundation under the President of the Republic of Azerbaijan (Grant No. EIF-BGM-4-RFTF- 1/2017-21 / 07/1).

A.Kh.is grateful for the support by the RFBR grant 19-02-00311 I.I.R. is grateful to the Russian Science Foundation for partial financial support of the work in terms of performing measurements of the magnetic fields of stars (grant from the Russian Science Foundation 21-12-00147).

REFERENCES

1. Bouwman J., de Koter A., van den Ancker M.E., and Waters L.B.F.M., Astron.Astrophys 2000, 360, 213

2. Sylvester R. J., Skinner C. J., Barlow M. J. and Mannings V., MNRAS 1996, 279, 915

3. SIMBAD-VizieR, 2012yCat.2311, 0C

4. https://irsa.ipac.caltech.edu/IRASdocs/e.p.sup/

5. Smith B. J., Price S. D., Baker R. I. ApJS, 2004, 54, 673

6. Johnson H.L., 1950, ApJ 112, 240

7. Straizis V. Multicolor photometry of stars. Mosklas, Vilnus,1977, .312

8. Ismailov N.Z. Practical Astrophysics, Baku, 2012, .180

9. Savage, B. D., and Mathis, J. D. 1979, Ann. Rev. Astr. Ap., 17, 73.

10. Rieke G. H., Lebofsky M. J. Astrophys.J., 1985, 288, 618

11. Nandy, K., Thompson, G. L, Jamar, C, Monfils, A., and Wilson, R. 1976, Astr.Ap., 51, 63

12. Schultz, G. V., and Wiemer, W. 1975, Astr. Ap., 43, 133

13. Van de Hulst, H. C. 1949, Rech. Astr. Obs. Utrecht, Vol. 11, Part 2

14. Neugebauer G., Leighton R. B. 1969, Two Micron Sky Survey, a Preliminary Catalog (NASA SP-3047; Washington: GPO)

15. Cutri R. M. 2003, Explanatory Supplement to the 2MASS All Sky Data Release (Pasadena: Caltech), http://www.ipac.caltech.edu/2mass/releases/allsky/doc/ explsup.html

16. Epchtein N., et al. 1999, AA, 349, 236

17. Beichman C. A., Neugebauer G., Habing H. J., Clegg P. E., Chester, T. J. 1988, Explanatory Supplement for the Infrared Astronomical Satellite Catalogs and Atlases (Washington: GPO)

18. Price S. D., et al. 1999, ASP Conf. Ser. 177, Astrophysics with Infrared Surveys: A Prelude to SIRTF, ed. M. D. Bicay, C. A. Beichman, R. M. Cutri, B. F. Madore (San Francisco: ASP), 394

19. Price S. D., Walker R. G. 1976, Interim Report, Air Force Geophysical Laboratory, Hanscom AFB (AFGL-TR-0208 Environmental Research Papers)

20. Hauser M. G., Kelsall T., Leisawitz D., Weiland J. 1998, COBE Diffuse Infrared Background Experiment (DIRBE) Explanatory Supplement, vers. 2.3 (Greenbelt: NASA)

21. Boggess, N. W., et al. 1992, ApJ, 397, 420

22. Beverly J. S., Stephan D. P., Rachel I. B. ApJS, 2004, 154, 673

23. Schlegel et al. 1998, ApJ 500, 525

24. Schlafly Finkbeiner 2011, ApJ 737, 103

25. Aumann et al.,1984, ApJ 278, L23-L27

26. Aumann H.H., 1985, PASP, 97, 885

27. Kurucz R.L, 1979, Astrophys.J.S., 40, 1

28. Moshir et al., 1990 IRASF.C.....0M. IRAS Faint Source Catalogue, version 2.0

29. Secrest N. J., Dudik R. P., Dorland B. N. et al., 2015ApJS, 221,12

30. Tie Liu, Huawei Zhang, Yuefang Wu et al., 2011, ApJ, 734, 22

31. Romanyuk I. I., Semenko E. A., Yakunin I. A., Kudryavtsev D. O., Chemically Peculiar Stars in the Orion OB1 Association. I. Occurrence Frequency, Spatial Distribution, and Kinematics, Astrophysical Bulletin 2013, 68, № 3, 318